Effect of Purification Method of β-Chitin from Squid Pen on the Properties of β-Chitin Nanofibers

Shin Suenaga[a], Nozomi Nikaido[b], Kazuhide Totani[b], Kazunori Kawasaki[c], Yoshihito Ito[d], Kazuhiko Yamashita[e], and Mitsumasa Osada[a,*]

[a] *Department of Chemistry and Materials, Faculty of Textile Science and Technology, Shinshu University, 3-15-1, Tokida, Ueda, Nagano 386-8567, Japan*

[b] *Department of Chemical Engineering, National Institute of Technology, Ichinoseki College, Takanashi, Hagisho, Ichinoseki, Iwate 021-8511, Japan*

[c] *National Institute of Advanced Science and Technology (AIST), 1-8-31, Midorigaoka, Ikeda, Osaka 563-8577, Japan*

[d] *Iwate Industrial Research Institute, 2-4-25, Kitaiioka, Morioka, Iwate 020-0857, Japan*

[e] *Yaegaki Bio-industry, Inc., 681, Mukudani, Hayashida, Himeji, Hyogo 678–4298, Japan*

Corresponding author. Phone: +81-268-21-5458; Fax: +81-268-21-5391

E-mail: osadam@shinshu-u.ac.jp

Abstract

The relationship between purification methods of β-chitin from squid pen and the physicochemical properties of β-chitin nanofibers (NFs) were investigated. Two types of β-chitin were prepared, with β-chitin (a→b) subjected to acid treatment for decalcification and then base treatment for deproteinization, while β-chitin (b→a) was treated in the opposite order. These β-chitins were disintegrated into NFs using wet pulverization. The β-chitin (b→a) NF dispersion has higher transmittance and viscosity than the β-chitin (a→b) NF dispersion. For the first time, we succeeded in obtaining 3D images of the β-chitin NF dispersion in water by using quick-freeze deep-etch replication with high-angle annular dark field scanning transmission electron microscopy. The β-chitin (b→a) NF dispersion has a denser and more uniform 3D network structure than the β-chitin (a→b) NF dispersion. Widths of the β-chitin (a→b) and (b→a) NFs were approximately 8–25 and 3–10 nm, respectively.

Keywords: Chitin, Nanofiber, Star Burst

1.Introduction

Chitin is long-chain polysaccharides consisting of β-(1-4)-linked *N*-acetyl anhydroglucosamine units, and has the potential for use in medical supplies, cosmetics, and food [1–3] owing to high biocompatibility [4,5]. Chitin is classified α-chitin or β-chitin, depending on its crystalline structure. Most chitin is purified from exoskeletons of crustaceans, cell walls of fungi and yeasts, etc. as α-chitin [6]. α-Chitin has antiparallel molecular chains with hydrogen bonds between the chains. On the other hand, β-chitin is purified from squid pens, tubeworm housing tubes, diatom spines, etc., and the lower natural abundance compared to α-chitin [7]. The anhydrous β-chitin has parallel molecular chains without significant hydrogen bonds between intermolecular sheets [8,9]. The residual proteins in α-chitin from crab and shrimp can possibly trigger shellfish allergies, while molluscan such as squid allergy does not appear to occur as frequently compared to crustacean allergy [10]. This means that β-chitin from squid pen is safer to utilize in human medical applications.

When α-chitin is purified from commercially available crab shell, acid treatment is performed first for decalcification, followed by base treatment for deproteinization. The later base treatment is believed to aid in base deacetylation for subsequent chitosan production. The purification of β-chitin from squid pen also requires acid and base treatments for decalcification and deproteinization. However, the relationship between the purification method used to obtain β-chitin from squid pen and the physicochemical properties of the resulting β-chitin nanofiber (NF) has not been reported. Therefore, investigations into the overall process going from the squid pen raw material to β-chitin NF are needed.

Chitin NF has attracted research interest in the field of materials chemistry [11,12].

When chitin is disintegrated into NF, the hydrophilic surface area increases, enhancing the biochemical significance of the material [13,14]. As disintegrating methods of chitin into NF, ultrasonication, grinding, or the Star Burst system under acidic conditions have been reported [15–17]. The Star Burst system can convert α-chitin and cellulose into their NFs by wet pulverization using a water jet [18]. This system uses only water without the need for additional acid, achieves much lower contamination, and has high throughput [19,20]. These advantages can reduce the barrier for use in medical supplies, cosmetics, and food. Therefore, we adopt the Star Burst system for disintegrating β-chitin into NF.

In this study, we prepared two types of β-chitin from squid pen, with β-chitin (a→b) subjected to acid treatment for decalcification and then base treatment for deproteinization, while β-chitin (b→a) was treated in the opposite order. The physicochemical properties of the β-chitin (a→b) and (b→a) NFs were characterized by XRD, transmittance, viscosity, and molecular weight measurement and electron microscopy. In particular, 3D images of β-chitin NF were obtained with quick-freeze deep-etch replication and high-angle annular dark field scanning TEM (HAADF-STEM) for the first time, in order to observe the state of NF dispersion. We revealed that relationship between purification methods of β-chitin and the physicochemical properties of β-chitin NF.

2. Materials and methods

2.1. Materials

Squid pen contains 30% β-chitin, 70% protein, and less than 1% ash [21,22]. Two types of β-chitin were prepared from a squid pen (*Todarodes pacificus*) by removing the

protein and ash (Fig. 1). The first one is β-chitin (a→b). 2 kg (wet weight) of squid pens were soaked in 0.1 mol L^{-1} hydrochloric acid solution (10 L) for 16 h at 15 °C to remove ash, and the pens were then washed four times with distilled water (20 L per wash). The decalcified squid pens were soaked in 1 mol L^{-1} sodium hydroxide solution (10 L) for 2 h at 90 °C to remove protein, and were then washed once with distilled water (20 L). The protein removal process was then repeated. Afterwards, the β-chitin was washed four times with distilled water (20 L per wash) until a neutral pH was reached in the bulk water.

To obtain β-chitin (b→a), squid pens were first treated twice with 1 mol L^{-1} sodium hydroxide solution and then treated with 0.1 mol L^{-1} hydrochloric acid solution. Afterwards, the β-chitin was washed four times with distilled water until a neutral pH was reached in the bulk water. The β-chitin (a→b) and β-chitin (b→a) were both dried at 65 °C for 16 h, and then ground to obtain particles less than 100 μm in diameter.

For comparison, α-chitin (< 100 μm diameter) was obtained from Yaegaki Bio-industry, Inc. and used without further purification.

2.2. Preparation of Chitin Nanofibers

The β-chitin (a→b) and β-chitin (b→a) powders were suspended separately in distilled water at 1 wt%. The slurries were disintegrated using a Star Burst system (Sugino Machine Co., Ltd.) (Fig. 2). The β-chitin slurries were pressurized from 230 to 240 MPa and then ejected from a nozzle (100 μm aperture). The β-chitin slurries were diagonally made to collide with each other. The disintegrated β-chitin was recovered after cooling with a heat exchanger. The number of collision times (= pass) was set to 2, 5, and 10 passes.

2.3. Elementary Analysis

To evaluate the degree of *N*-acetylation, the amount of nitrogen and carbon in the β-chitin (a→b) and β-chitin (b→a) powders were measured using an element analyzer (Sumika Chemical Analysis Service, Ltd., SUMIGRAPH NC-1000). Acetanilide was used as a reference material. The degrees of *N*-acetylation were calculated from the following equation:

Degrees of *N*-acetylation = $(C/N - 6) / 2$ (1)

where *C* is moles of carbon and *N* is moles of nitrogen.

2.4. X-ray Diffraction (XRD)

The 1 wt% β-chitin (a→b) and (b→a) NF dispersions were dried at 75°C for 12 h. The β-chitin (a→b), β-chitin (b→a), and α-chitin powder and their NFs (except α-chitin) were converted into pellets approximately 1.3 cm in diameter and approximately 0.43 mm in thickness by pressing at approximately 750 MPa for 1 min using a hand-press machine (Shimadzu Co., Ltd., SSP-10A). XRD patterns of the β-chitin (a→b) and β-chitin (b→a) powder and NF were measured from 5–35° of diffraction angle 2θ (in radians) using an X-ray diffractometer (Rigaku Co., Ltd., RINT 2500HF/PC) with Cu-Kα radiation at 40 kV and 40 mA. The crystallinity index (CI) was determined by the following equation:

CI = $(I_{1\text{-}10} - I_{am}) / I_{1\text{-}10}$ (2)

where I_{1-10} is the maximum intensity of the [1−10] mixed plane and I_{am} is the intensity of the amorphous diffraction at 16° [23]. *d*-Spacing was determined using Bragg's law, which states that

d-Spacing [Å] = λ / 2 sinθ (3)

where λ is the wavelength of Cu-Kα radiation (λ = 1.5418 Å) and θ (in radians) is the

scattering angle.

2.5. Fourier Transform Infrared (FT-IR) Spectroscopy

The β-chitin (a→b) and β-chitin (b→a) powder were blended with potassium

chloride and converted into pellet using a mini hand-press machine (Shimadzu Co.,

Ltd., MHP-1). We did not use potassium bromide because the bromine affects FT-IR

spectra by ion-exchange with residual chlorine combined with amino group of the β-

chitin (b→a) powder after acid treatment. FT-IR spectra of the pellet were recorded

using an FT-IR spectrometer (JASCO Co., Ltd., FT/IR 4200) from 500 to 4000 cm^{-1}

with 4 cm^{-1} resolution and 32 scans.

2.6. Molecular Weight Distribution

The molecular weight distributions of the β-chitin (a→b) and β-chitin (b→a) NFs

were measured using a gel permeation chromatography (GPC) system (Shimadzu, SCL-

10Avp), which was equipped with a refractive index detector, a GPC column (Showa

Denko K. K., Shodex GPC KD-806K + KD-803), and a guard column (Showa Denko

K. K., Shodex GPC KD-G). Pullulan standards (Showa Denko K. K., Shodex

STANDARD P-82) of 708, 340, 200, 107, 47.1, 21.1, 9.6, and 5.9 kDa were used. A

total of 1% of the sample was dissolved in a 5% LiCl/DMAC solution with continuous

stirring for 2 days. Prior to measurement, the samples were filtered through a 0.45 μm

nylon filter. The flow rate of the mobile phase was 0.5 mL min^{-1}. The temperatures of

the columns and the detector were set at 50 °C. A calibration curve was plotted for the

elution time versus the absolute molecular weight of the standards, and the relative molecular weight of the β-chitin samples was estimated from the standard curve.

2.7. Optical Transmittance

The 1 wt% β-chitin NF dispersions were diluted with distilled water to 0.05 wt% and sonicated for 20 minutes using an ultrasonic washing machine (SND Co., Ltd., USK-4). The 0.05 wt% β-chitin dispersions were then loaded into quartz cuvettes. The transmittance was measured over a range of 200–700 nm by a spectrophotometer (JASCO Co., Ltd., V-630 BIO), using distilled water as a blank.

2.8. Viscoelastic Measurements

The 1 wt% β-chitin NF dispersions were loaded into 35 mL glass bottles. The β-chitin dispersions were placed in a thermostat chamber filled with water at 25 °C, and the viscosity was measured with a Brookfield viscometer (Brookfield Asset Management Inc., DIGITAL VISCOMETER MODEL DV-2). First, a #64 spindle was used at a viscosity of more than 1000 mPa·s. A #62 spindle was then used at a viscosity of less than 1000 mPa·s. These measurements were carried out at a rotational speed of 50 rpm for 500 s.

2.9. Quick-Freeze Deep-Etch Replication and High-Angle Annular Dark Field Scanning Transmission Electron Microscopy (HAADF-STEM)

The 1 wt% β-chitin NF dispersions were frozen using a metal contact method; the dispersions were brought into contact with a pure copper block cooled by liquid helium. The frozen sample was cut at from –85 to –90 °C. The cut section was freeze-dried to

etch the ice, exposing the β-chitin NF. The etched surface was coated with an approximately 6.5 nm layer of platinum and carbon as a replica membrane, and then coated with an approximately 27 nm layer of carbon to reinforce the replica membrane. The coated sample was soaked in a formic acid overnight to eliminate the β-chitin NF, so that only the replica membrane remained. After the replica membrane was washed with water, it was mounted on a grid. The sample was studied using a HAADF-STEM (FEI, Tecnai G2F20) operating at 200 kV. When the width of the β-chitin NF was estimated, we subtracted the thickness of the platinum layer from the NFs images observed by the HAADF-STEM.

2.10. Field-Emission Scanning Electron Microscopy (FE-SEM)

A β-chitin NF dispersion was precipitated with a centrifuge, and the supernatant was removed. We added *tert*-butyl alcohol to the precipitate, which was subsequently dispersed using ultrasonication. After repeating this process several times, the solvent was exchanged from water to *tert*-butyl alcohol. This mixture was then frozen at −80 °C and dried under vacuum. The dried β-chitin NF was coated with an osmium tetroxide layer approximately 3 nm in thickness. The sample was viewed using an FE-SEM (JEOL, JSM-7001F) operating at 2.0 kV.

2.11. Transmission Electron Microscopy (TEM)

The 1 wt% β-chitin NF dispersions were diluted with distilled water to 0.02 wt% and sonicated for 20 min using an ultrasonication. A drop of the dispersion was mounted on a carbon coated micro grid. After approximately 1 min, the excess liquid was absorbed by a filter paper. A concave background was stained a drop of 2% uranyl

acetate for 5 min, and the excess solution was drawn off the micro grid using filter paper. The negatively stained sample was left in air to dry. The sample was observed at 80 kV by a TEM (JEOL, JEM-2100).

3. Results

3.1. Characterization of Purified β-Chitin Powder

Before grinding to the powders, the purified β-chitin (a→b) was flexible to the touch, but the purified β-chitin (b→a) was more fragile. As mentioned in the *2.1.* Section, the pH of bulk water was neutral at the final washing treatment of the purified β-chitin. However, the pH of the distilled water added to the β-chitin (b→a) powder was slightly acidic (pH ≈ 4), while on the other hand, the pH in the case of the β-chitin (a→b) powder was about 7–8. The degree of *N*-acetylation in both β-chitin (a→b) and β-chitin (b→a) powder were the same (0.96 ± 0.03). The residual proteins in both β-chitin (a→b) and β-chitin (b→a) powders were about 0.08 and 0.16 wt%, respectively (refer to Supplementary data). Therefore, the residual proteins almost did not affect the degree of *N*-acetylation. XRD patterns of both β-chitin powders (Fig. 3) are almost the same and exhibit two diffraction peaks at 8.5 and 19.7°, which correspond to the [010] plane and [1–10] mixed plane, respectively. These results were similar to that of a β-chitin powder reported previously [24]. The CI and *d*-spacing of the β-chitin (a→b) powder were almost the same as those found in the β-chitin (b→a) powder (Fig. 3). XRD patterns of the α-chitin powder is also shown in Fig. 3 and five diffraction peaks at 9.3, 19.3, 20.9, 23.2, and 26.2°, corresponding to the [020], [110], [120], [130], and [013] planes, respectively, were observed [6]. FT-IR spectra of both β-chitins are almost

the same as shown in Fig. 4, and matched that of β-chitin reported previously [24].

3.2. Characterization of β-Chitin NF

The XRD patterns of β-chitin (a→b) and β-chitin (b→a) NFs (Fig. 3) were nearly

identical to those of the β-chitin powders, indicating that the β-chitin crystal structure

was maintained. However, the CIs of the β-chitin (a→b) and β-chitin (b→a) NFs were

slightly greater than in the corresponding β-chitin powders. In addition, the peak of the

[010] plane of both β-chitin NFs was shifted from about 8.5° to 9.0°, indicating a

decrease in the *d*-spacing at the [010] plane from about 10.4 Å to 9.8 Å.

Although the XRD patterns between β-chitin (a→b) and β-chitin (b→a) NFs were

almost the same, there were clear differences on the transmittances and the viscosities

between β-chitin (a→b) and β-chitin (b→a) NFs as follows.

The transmittances of the β-chitin (a→b) and β-chitin (b→a) NF dispersions at 0.05

wt% were shown in Fig. 5. The transmittance of both dispersions was increased by

increasing the pass time. The transmittance of β-chitin (a→b) NF dispersions was less

than 80% at 10 passes, while the transmittance of β-chitin (b→a) NF dispersions

reached to 80% at only 5 passes. The β-chitin (b→a) powder was disintegrated into a

homogeneous NF dispersion more easily than the β-chitin (a→b) powder.

The viscosities of the β-chitin (a→b) and β-chitin (b→a) NF dispersions at 1 wt%

are shown in Table 1. The viscosity of the β-chitin (b→a) was similar to what has been

previously reported [17]. The viscosity of both dispersions was decreased by increasing

the pass time. The viscosity of the β-chitin (b→a) NF was 6–8 times higher than that of

the β-chitin (a→b) NF. The β-chitin (a→b) NF dispersion was pulpy and ran off easily

when inverted in a container. By contrast, the β-chitin (b→a) NF dispersion had a more gel-like character and did not run off when inverted.

The molecular weights of the NF dispersions of β-chitin (a→b) and (b→a) are shown in Table 1. The molecular weight of the β-chitin (b→a) NF was smaller than that of β-chitin (a→b) NF for all pass times.

3.3. The State of β-Chitin NF Dispersions in Water

The state of β-chitin NF dispersions was observed by 3 ways, namely HAADF-STEM, FE-SEM, and TEM. HAADF-STEM images are 3D, on the other hand, FE-SEM and TEM images are 2D.

HAADF-STEM images of the β-chitin (a→b) and β-chitin (b→a) are shown in the upper row of Fig. 6. HAADF-STEM 3D images were obtained as videos in this study, and are available in the Supplementary data (Videos S1–4). The width of the β-chitin (a→b) NF at 2 passes was approximately 10–25 nm, and thick fibers of over 100 nm in width were also observed. The width of the β-chitin (a→b) NF at 10 passes was approximately 8–25 nm. The width of the β-chitin (b→a) at 2 passes was approximately 3–15 nm. The width of the β-chitin (b→a) NF at 10 passes was approximately 3–10 nm. The width of both NFs at 10 passes were thinner and more uniform than in the case of 2 passes, and in particular the 3D network structure of the fine β-chitin (b→a) NF was uniform and dense. The depth of the replica β-chitin (a→b) NF and β-chitin (b→a) NF at 10 passes were 610 and 280 nm, respectively.

FE-SEM images of the β-chitin (a→b) and β-chitin (b→a) NFs are shown in the middle row of Fig. 6. The width of the β-chitin (a→b) NF at 2 passes was

approximately 20–60 nm, and did not disperse uniformly. Furthermore, thick fibers over 100 nm in width were also observed. The width of the β-chitin (a→b) NF at 10 passes was approximately 10–50 nm and was more uniform than in the case of 2 passes. In contrast, the β-chitin (b→a) dispersed uniformly at only 2 passes, and the width of the β-chitin (b→a) NF was approximately 6–20 nm. The width of the β-chitin (b→a) NF at 10 passes was the same as that at 2 passes.

TEM images of the β-chitin (a→b) and β-chitin (b→a) NFs are shown in the bottom row of Fig. 6. These TEM images show the width of individual NFs within the dispersions. The width of β-chitin (a→b) NF at 2 passes was approximately 100–300 nm, and after 10 passes it was approximately 8–20 nm. The width of β-chitin (b→a) at 2 passes was approximately 4–7 nm and approximately 5–10 nm at 10 passes.

4. Discussion

For the β-chitin powders, the results of degrees of *N*-acetylation, XRD, and FT-IR indicated that the crystal and chemical structures were basically indifferent to the order of the acid and base treatments. However, for the β-chitin NFs, the increase of CI and the decrease of the *d*-spacing at the [010] plane occurred that were not observed in the β-chitin powders. The increase of CI is likely due to the rearrangement of the NF. When the β-chitin NFs were dried for XRD analysis, the β-chitin NFs would adhere to each other, arranging the contact surface of the NFs. The decrease of the *d*-spacing at the [010] plane is likely due to the desorption of water from the β-chitin crystal structure. When the crystal structure of the β-chitin was changed from the dihydrate to the anhydrous form, the *d*-spacing at the [010] plane decreased from about 11.03 Å to 9.14 Å [25]. In this work, the *d*-spacing of about 10.4 Å (i.e. the diffraction at 8.5°) is a

typical of the monohydrate crystal. On the other hand, the *d*-spacing of about 9.8 Å (i.e. the diffraction at 9.0°) observed in the β-chitin NFs would be derived from the intermediate structure between the monohydrate and the anhydrous form. When the β-chitin NFs were dried, the water molecule would be desorbed easier than in the corresponding β-chitin powders because the β-chitin NFs have larger surface area.

The molecular weight of the β-chitin (a→b) NF was greater than that of the β-chitin (b→a) NF for all pass times, which is likely due to residual HCl in the purified β-chitin (b→a). As mentioned in the *3.1*. Section, the pH of the distilled water added to the β-chitin (b→a) powder was slightly acidic (pH ≈ 4), while the pH in the case of the β-chitin (a→b) powder was about 7–8. This is because the protons are released from the β-chitin (b→a) molecular chains when its powder was soaked in water. In additional experiments shown in the Supplementary data, we washed the β-chitin (b→a) powder with additional water until the pH of the bulk material reached neutral. As a result, the physicochemical properties of the washed β-chitin (b→a) NF were similar to those of the β-chitin (a→b) NF, indicating that HCl remained in the β-chitin (b→a) powder. It has been reported that β-chitin can have small molecules (such as water and HCl) between the β-chitin molecular chains [26–28]. When the purified β-chitin (b→a) was dried at 65 °C, the HCl in β-chitin was condensed. Condensed and heated HCl can potentially cleave glycosidic bonds in β-chitin (i.e. hydrolysis). As a result, the molecular weight of the β-chitin (b→a) NF became smaller than that of the β-chitin (a→b) NF.

From the HAADF-STEM observation, the β-chitin (b→a) NF was thinner than the β-chitin (a→b) NF at 2 passes, and all β-chitin (b→a) NFs were less than 100 nm. The

14

thinner β-chitin (b→a) would be due to electrostatic repulsions. The β-chitin powder consists of an assembly of the β-chitin NFs [29]. The β-chitin (b→a) powder is expected to be cationized due to protons derived from residual HCl between the β-chitin (b→a) molecular chains. The electrostatic repulsions between NFs assembled in the cationized β-chitin (b→a) powder promoted to disintegrate the powder into NFs, therefore, the β-chitin (b→a) NF was less than 15 nm at 2 passes. The residual HCl also increased the local concentration of H^+ and Cl^- ions between β-chitin (b→a) NFs after disintegration. To balance the osmotic pressure, the bulk water moves between the β-chitin (b→a) NFs, resulting that the β-chitin (b→a) NFs could keep uniform and high dispersion. On the other hand, the β-chitin (a→b) was not cationized, resulting that there was not the electrostatic repulsion. For β-chitin (a→b), the energy given by the Star Burst system at 2 passes was not enough to disintegrate the all powder into NFs less than 100 nm, while it would be enough at 10 passes.

The viscosity of the β-chitin (b→a) NF was higher than that of the β-chitin (a→b) NF, while the molecular weight of the β-chitin (b→a) NF was lower than that of the β-chitin (a→b) NF as shown in Table 1. In general, the viscosity of dissolved polymers is reduced as the decrease of the molecular weight [30]. As mentioned above, the β-chitin (b→a) and (a→b) NF were not dissolved in water but they dispersed with maintaining their crystal structure. From HAADF-STEM and FE-SEM observations, the width of the β-chitin (b→a) NF was thinner and more uniform than that of the β-chitin (a→b) NF, indicating that entanglements of the β-chitin (b→a) NFs were higher than those of the β-chitin (a→b) NFs. The higher entanglements between the β-chitin (b→a) NFs caused the higher viscosity.

The transmittance of the β-chitin (b→a) NF was higher than that of the β-chitin (a→b) NF as shown in Fig. 5. From HAADF-STEM and FE-SEM observations of the β-chitin (a→b) NF at 2 passes in Fig. 6, the NFs did not disperse uniformly and thick fibers over 100 nm in width were also observed. There are both dense and sparse spots of the β-chitin (a→b) NF. The refraction and reflection of light occur because the refractive indices of β-chitin and water are different, resulting that the transmittance of the β-chitin (a→b) NF became low. On the other hand, the fine and uniform 3D network structure of the β-chitin (b→a) NF inhibited the light scattering, resulting in an increase of the transmittance.

For the first time, we were able to observe 3D images of the β-chitin NF dispersions in water using quick-freeze deep-etch replication and HAADF-STEM. This method has several advantages over more conventional FE-SEM and TEM techniques, as this method can describe the NF dispersion in water due to the freezing sample on the millisecond timescale [31] and reinforcement with a carbon layer, which inhibits NF aggregation. Moreover, this method more accurately reflects the NF concentration. Conversely, conventional FE-SEM methods require pretreatment (e.g. substitution of dispersion medium and centrifugation or hot pressing) before observation. These pretreatments would change the state and shape of NF dispersion. As a result, large amorphous masses are often observed when using FE-SEM, which cannot be classified as to whether not the β-chitin disintegrated or aggregated by centrifuging. For TEM observations, diluting the NF dispersion is a necessary pretreatment step. TEM observations are better suited to determine tertiary structures (i.e. width and length of NF), but they are disadvantageous in regards to quaternary structures (i.e. the state of NF dispersion). Furthermore, the accurate NF concentration is unknown in FE-SEM and

TEM observations due to pretreatment. Therefore, the quick-freeze deep-etch replication and HAADF-STEM observation method is a promising method to investigate the actual NF state in water.

On the HAADF-STEM (Fig. 6, Video S3, and Video S4), the depth of the β-chitin (b→a) NF replica was thinner than that of the β-chitin (a→b). When the quick-freeze deep-etch replication process is carried out with the same drying time, the depth of the replica depends on capacity for water retention of sample. If water hardly sublimes, 3D replica becomes thin, indicating that the thin sample has a high capacity for water retention. Therefore, the β-chitin (b→a) NF has better water retention than the β-chitin (a→b) NF; as the dense structure of the β-chitin (b→a) NF traps water in this 3D network structure.

5. Conclusions

We revealed the effect of the purification treatment order of β-chitin from squid pen on the physicochemical properties of the β-chitin NF. Two types of β-chitin were prepared, with the β-chitin (a→b) treated by acid and base (in order) and the β-chitin (b→a) treated in the opposite order. For the powder form, the chemical and crystal structures of the β-chitin were almost the same regardless of treatment order. However, in the NF form, the treatment order significantly affected the physicochemical properties of the NFs. The β-chitin (b→a) NF dispersion showed higher transmittance and higher viscosity than the β-chitin (a→b) NF dispersion. In addition, we have demonstrated 3D image analysis of the β-chitin NF dispersions for the first time and it showed the dispersion state of β-chitin (b→a) NF was a denser and more uniform in

water than that of the β-chitin (a→b) NF. The width of the β-chitin (b→a) NF was

approximately 3–10 nm and that of the β-chitin (a→b) NF was approximately 8–25 nm

at 10 passes. For the β-chitin (b→a), residual HCl in the β-chitin crystals was released

to elutriation, which then cationized the β-chitin NFs. The cationized β-chitin (b→a)

NFs have the electrostatic repulsions each other, resulting in an increase of the

dispersibility, transmittance, and viscosity.

Acknowledgements

References

[1] Y. Maeda, R. Jayakumar, H. Nagahama, T. Furuike, H. Tamura, Int. J. Biol.
Macromol. 42 (2008) 463–467.

[2] S. Gautier, E. Xhauflaire-Uhoda, P. Gonry, G.E. Pierard, Int. J. Cosmet. Sci. 30
(2008) 459–469.

[3] L.K. Han, Y. Kimura, H. Okuda, Int. J. Obes. 23 (1999) 174–179.

[4] R. Jayakumar, M. Prabaharan, S.V. Nair, H. Tamura, Biotechnol. Adv. 28 (2010)
142–150.

[5] B. Ding, J. Cai, J. Huang, L. Zhang, Y. Chen, X. Shi, Y. Du, S. Kuga, J. Mater.
Chem. 22 (2012) 5801–5809.

[6] P. Sikorski, R. Hori, M. Wada, Biomacromolecules 10 (2009) 1100–1105.

[7] D. Sawada, Y. Nishiyama, P. Langan, V. T. Forsyth, S. Kimura, M. Wada, PLoS One
7 (2012) e39376.

[8] Y. Nishiyama, Y. Noishiki, M. Wada, Macromolecules 44 (2011) 950–957.

[9] D. Sawada, Y. Nishiyama, P. Langan, V.T. Forsyth, S. Kimura, M. Wada,
Biomacromolecules 13 (2012) 288–291.

[10] C. Unterberger, F. Luber, A. Demmel, K. Gruenwald, I. Huber, K.-H. Engel, U.
Busch, Eur. Food Res. Technol. 239 (2014) 559–566.

[11] C. Chen, D. Li, H. Yano, K. Abe, Cellulose 21 (2014) 3339–3346.

[12] I.F. Nata, S.S.-S. Wang, T.-M. Wu, C.-K. Lee, Carbohydr. Polym. 90 (2012) 1509–
1514.

[13] R. Izumi, S. Komada, K. Ochi, L. Karasawa, T. Osaki, Y. Murahata, T. Tsuka, T.
Imagawa, N. Itoh, Y. Okamoto, H. Izawa, M. Morimoto, H. Saimoto, K. Azuma, S.
Ifuku, Carbohydr. Polym. 123 (2015) 461–467.

[14] K. Azuma, T. Osaki, T. Wakuda, S. Ifuku, H. Saimoto, T. Tsuka, T. Imagawa, Y. Okamoto, S. Minami, Carbohydr. Polym. 87 (2012) 1399–1403.

[15] Y. Fan, H. Fukuzumi, T. Saito, A. Isogai, Int. J. Biol. Macromol. 50 (2012) 69–76.

[16] S. Ifuku, M. Nogi, K. Abe, M. Yoshioka, M. Morimoto, H. Saimoto, H. Yano, Biomacromolecules 10 (2009) 1584–1588.

[17] A.K. Dutta, H. Izawa, M. Morimoto, H. Saimoto, S. Ifuku, Journal of Chitin and Chitosan Science 1 (2013) 186–191.

[18] R. Kose, T. Kondo, Sen'i Gakkaishi. 67 (2011) 91–95.

[19] S. Ifuku, K. Yamada, M. Morimoto, H. Saimoto, J. Nanomater. 2012 (2012) 1–7.

[20] Y. Watanabe, S. Kitamura, K. Kawasaki, T. Kato, K. Uegaki, K. Ogura, K. Ishikawa, Biopolymers 95 (2011) 833–839.

[21] S. Hunt, M. Nixon, Comp. Biochem. Physiol., Part B: Biochem. Mol. Biol. 68B (1981) 535–546.

[22] D.K. Youn, H.K. No, W. Prinyawiwatkul, Int. J. Food Sci. Technol. 48 (2013) 571–577.

[23] Y. Zhang, C. Xue, Y. Xue, R. Gao, X. Zhang, Carbohydr. Res. 340 (2005) 1914–1917.

[24] Y. Fan, T. Saito, A. Isogai, Biomacromolecules 9 (2008) 1919–1923.

[25] K. Kobayashi, S. Kimura, E. Togawa, M. Wada, Carbohydr. Polym. 79 (2010) 882–889.

[26] Y. Saito, J.-L. Putaux, T. Okano, F. Gaill, H. Chanzy, Macromolecules 30 (1997) 3867–3873.

[27] J. Blackwell, Biopolymers 7 (1969) 281–298.

[28] Y. Saito, T. Okano, F. Gaill, H. Chanzy, J.-L. Putaux, Int. J. Biol. Macromol. 28

(2000) 81–88.

[29] F.-C. Yang, R.D. Peters, H. Dies, M.C. Rheinstadter, Soft Matter 10 (2014) 5541–5549.

[30] M. Terbojevich, C. Carraro, A. Cosani, E. Marsano, Carbohydr. Res. 180 (1988) 73–86.

[31] T. Nakata, K. Sobue, N. Hirokawa, J. Cell Biol. 110 (1990) 13–25.

Appendix A. Supplementary data

Further information on residual proteins in the purified β-chitin can be found in S−1 and Table S1. The HAADF-STEM 3D videos of the 1 wt% β-chitin (a→b) (Videos S1 and S3) and β-chitin (b→a) (Videos S2 and S4) NF dispersions at 10 passes are available. Further information on residual HCl in the β-chitin (b→a) can be found in S−3 and Figs. S1−3. Their data can be found, in the online version.

Tables

Table 1. The viscosity at 1 wt% and the molecular weights of the β-chitin (a→b) and (b→a) NF dispersions.

Sample	Pass times	Viscosity (mPa·s)	Molecular weights (kDa)
β-chitin (a→b)	2	490	1800
	5	330	1730
	10	310	1450
β-chitin (b→a)	2	3100	1150
	5	2700	1240
	10	2000	1180

Figure Captions

Fig. 1. Purification methods of the β-chitin (a→b) and (b→a) from squid pen.

Fig. 2. Wet pulverization system using a water jet, also referred to as the Star Burst system.

Fig. 3. X-ray diffraction patterns of the β-chitin (a→b), (b→a), and α-chitin powder and their NFs (except for α-chitin). CI is crystallinity index (see Eq. 2), and d is d-spacing at [010] plane (for α-chitin powder, d-spacing at [020] plane).

Fig. 4. FT-IR spectra of the β-chitin (a→b) and (b→a) powders.

Fig. 5. The transmittance spectra of the β-chitin (a→b) and (b→a) NF dispersions at 0.05 wt%

Fig. 6. Images of the NF dispersions of the β-chitin (a→b) and (b→a). In HAADF-STEM, β-chitin NF dispersions was 1 wt%.

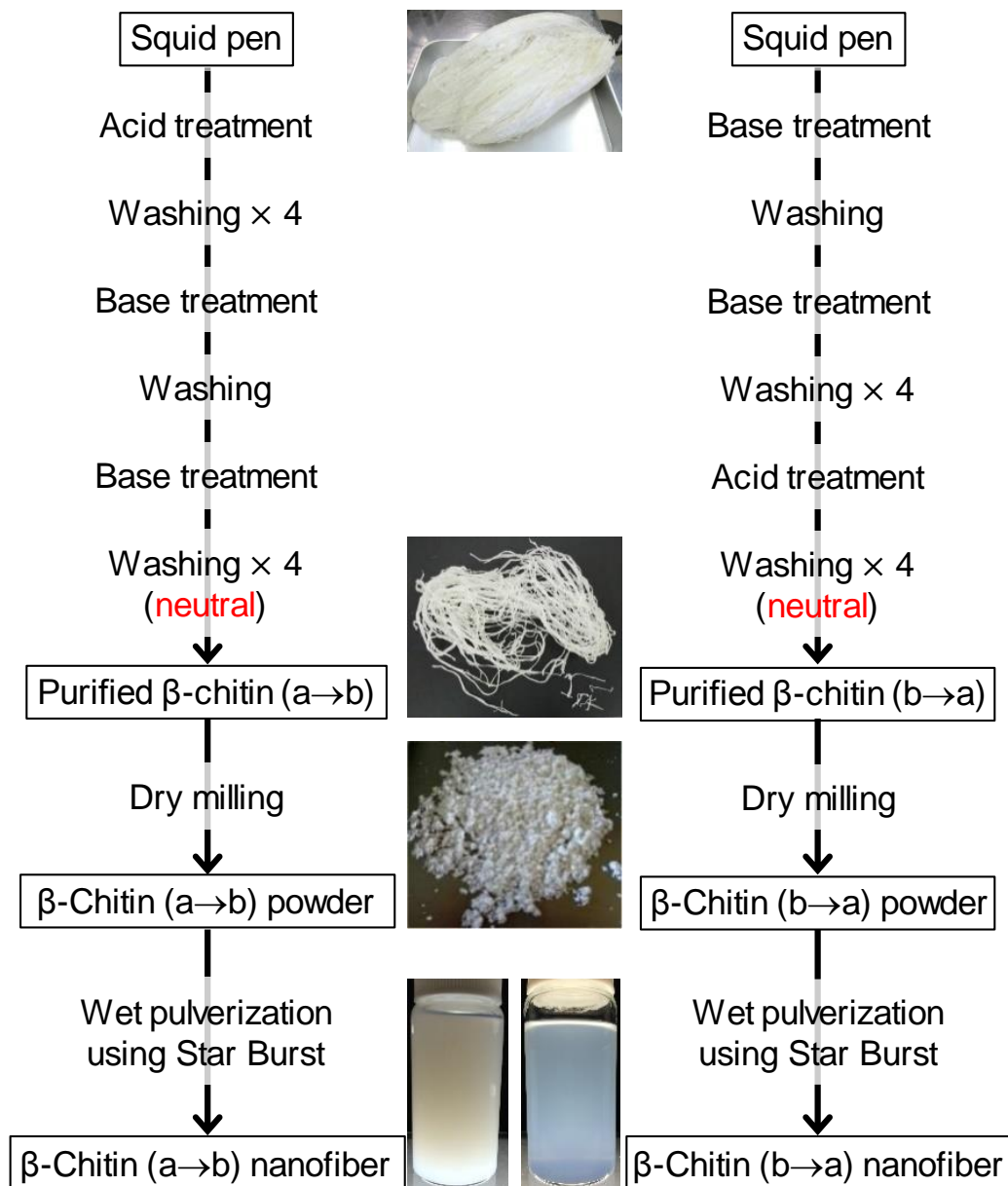| Squid pen		Squid pen
Acid treatment		Base treatment
Washing × 4		Washing
Base treatment		Base treatment
Washing		Washing × 4
Base treatment		Acid treatment
Washing × 4 (neutral)		Washing × 4 (neutral)
Purified β-chitin (a→b)		Purified β-chitin (b→a)
Dry milling		Dry milling
β-Chitin (a→b) powder		β-Chitin (b→a) powder
Wet pulverization using Star Burst		Wet pulverization using Star Burst
β-Chitin (a→b) nanofiber		β-Chitin (b→a) nanofiber

Fig. 1. S. Suenaga et al.

Sample tank

Plunger

Nozzles
diameter 100 μm

**Slurry
in**

Super-high-pressure
filter

Heat exchanger

Feed pump

Chamber

**Sample
out**

Plunger

Fig. 2. S. Suenaga et al.

Fig. 3. S. Suenaga et al.
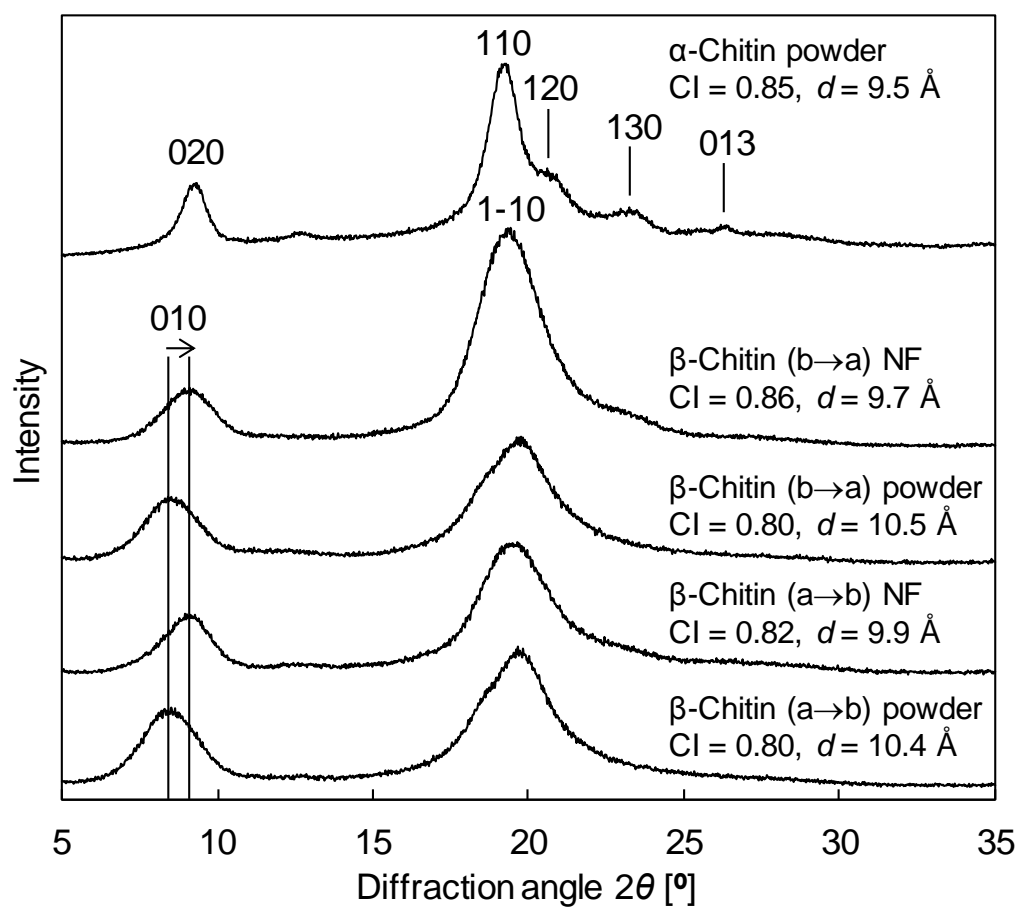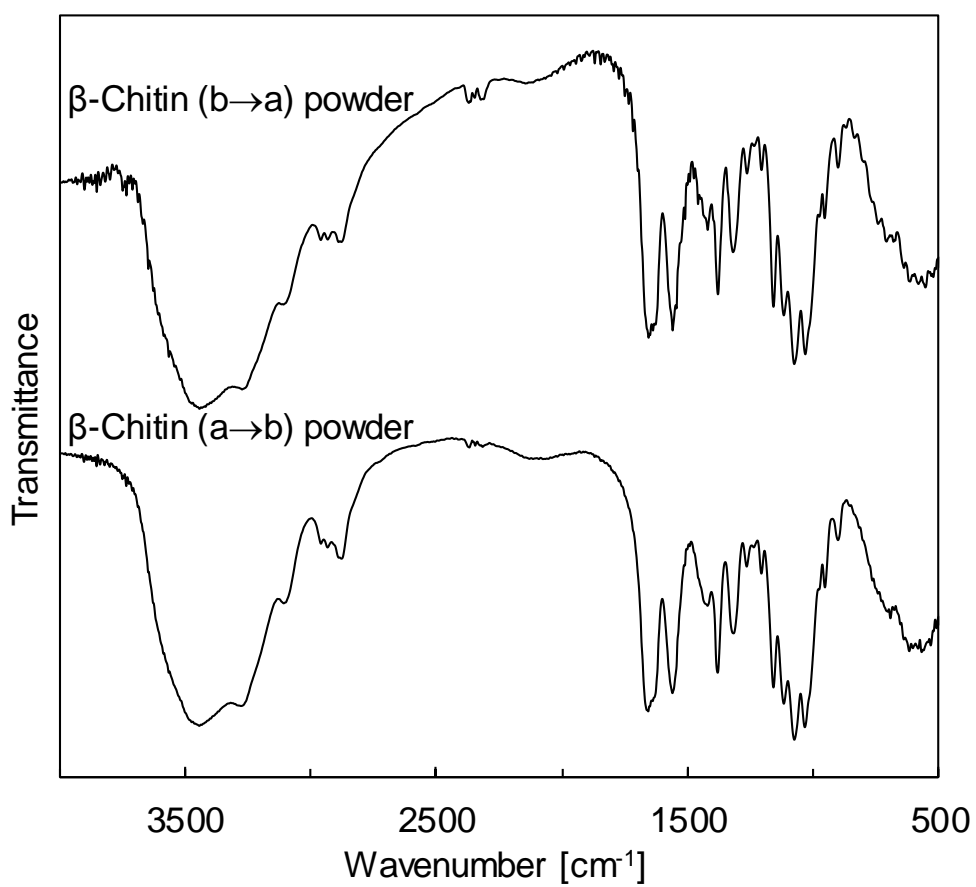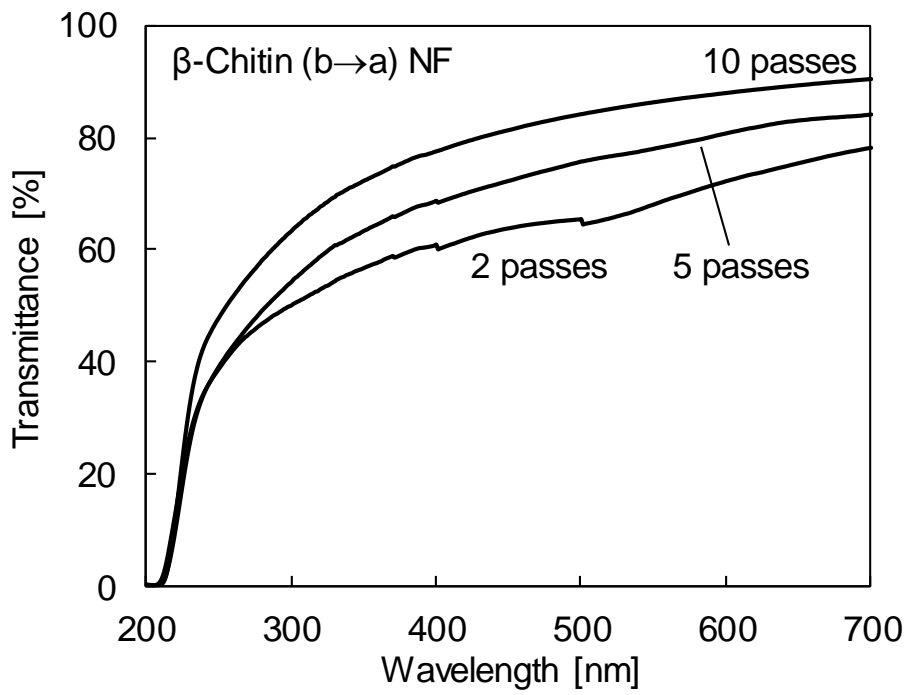
β-Chitin (b→a) powder

β-Chitin (a→b) powder

Transmittance

Wavenumber [cm⁻¹]

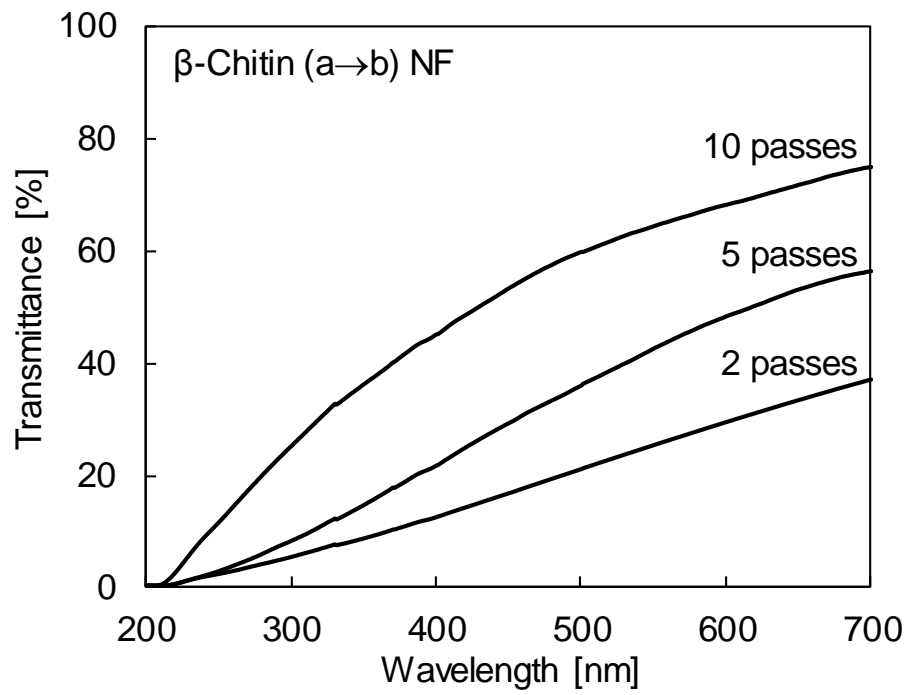Fig. 4. S. Suenaga et al.

Fig. 5. S. Suenaga et al.

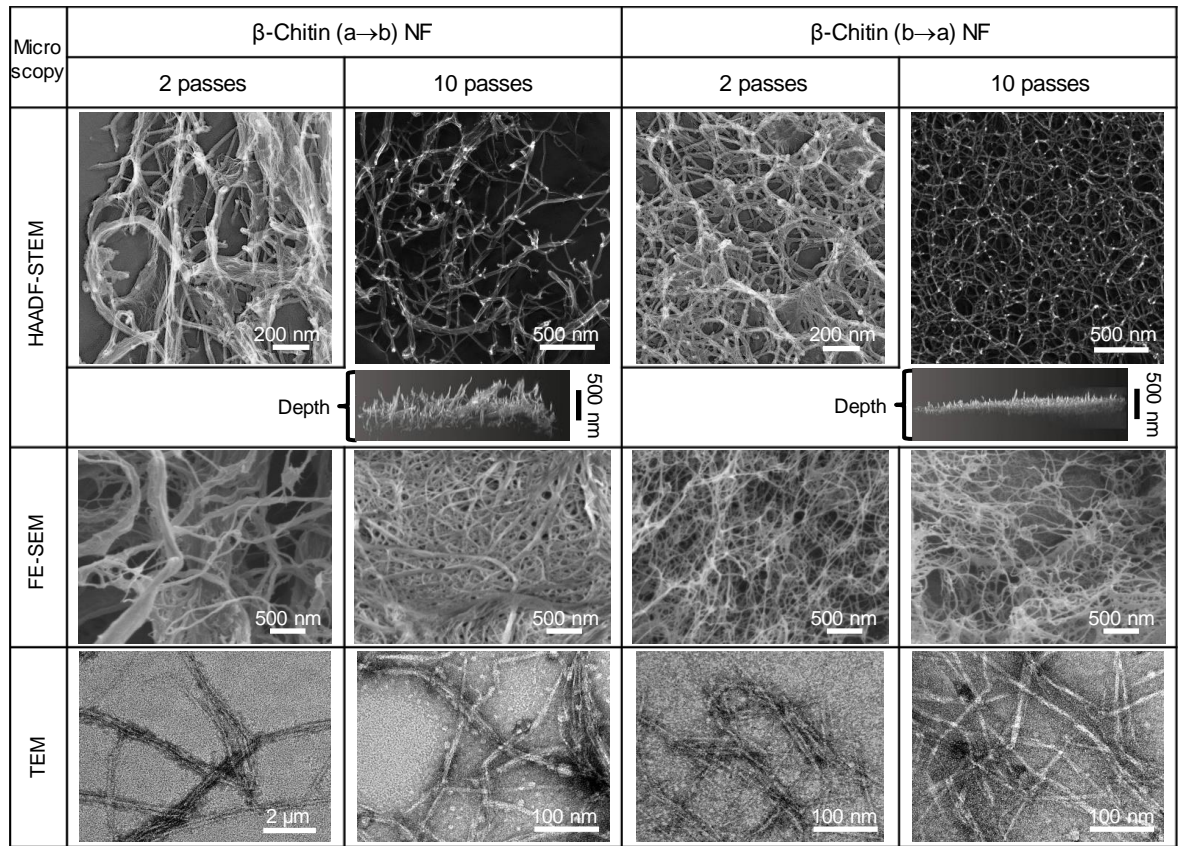| Micro scopy	β-Chitin (a→b) NF		β-Chitin (b→a) NF	
	2 passes	10 passes	2 passes	10 passes
HAADF-STEM	200 nm	500 nm	200 nm	500 nm
		Depth 500 nm		Depth 500 nm
FE-SEM	500 nm	500 nm	500 nm	500 nm
TEM	2 μm	100 nm	100 nm	100 nm

Fig. 6. S. Suenaga et al.